Alzheimer's Research & Therapy

RESEARCH

Open Access

Exploring neural correlates of automated speech-based cognitive markers through resting-state functional connectivity in aging and at-risk Alzheimer's disease

Qingyue Li[1*], Zampeta-Sofia Alexopoulou[2], Martin Dyrba[3], Elisa Mallick[4], Johannes Tröger[4], Eike Spruth[5,6], Slawek Altenstein[5,6], Claudia Bartels[7], Wenzel Glanz[8,9], Enise I. Incesoy[8], Michaela Butryn[8,9], Ingo Kilimann[3], Sebastian Sodenkamp[10,11], Franziska Maier[12], Ayda Rostamzadeh[12], Antje Osterrath[13,14], Josef Priller[5,6,15,16], Anja Schneider[17,18], Jens Wiltfang[7,19,20], Christoph Laske[10,11], Björn Falkenburger[13,14], Michael Wagner[17,18], Emrah Duezel[8,9], Annika Spottke[17,21], Gabor C. Petzold[17,22], Frank Jessen[12,17,23], Alexandra König[2,4,24], Stefanie Köhler[3], Stefan Teipel[1,3] and DELCODE, DESCRIBE study groups

Abstract

Background Digital speech-based assessments provide scalable tools for detecting subtle cognitive decline. Here, we investigated whether digitally derived speech-based composite score of cognition and individual speech features were associated with alterations in functional connectivity (FC) within task-related brain networks in the Alzheimer's disease spectrum, which are known to reflect cognitive performance and disease-related changes.

Methods Data were analyzed from 129 participants of the German PROSPECT-AD study, ranging from cognitively healthy individuals to those with mild cognitive impairment. Speech-based cognitive scores and speech features were derived from automated phone-administered semantic verbal fluency (SVF) and verbal learning tasks (VLT). Resting-state fMRI assessed FC, with intrinsic connectivity networks identified via independent component analysis and dual regression. Associations were examined using permutation-based voxel-wise regression, controlling for demographic and clinical covariates. Seed-to-voxel analyses were conducted to support network identification and complement findings.

Results Greater language network connectivity in the left middle temporal gyrus was associated with increased SVF temporal cluster switching (FWE < .05, cluster size = 12 voxels, mean T = 3.86). Exploratory analyses (uncorrected $p < .01$) demonstrated no significant associations between cognitive composite scores and FC. However, individual SVF and VLT speech features exhibited network-specific associations across executive, language, and default mode networks, indicating exploratory yet spatially distinct connectivity patterns.

*Correspondence:
Qingyue Li
Qingyue.Li@med.uni-rostock.de

Full list of author information is available at the end of the article

© The Author(s) 2026. **Open Access** This article is licensed under a Creative Commons Attribution 4.0 International License, which permits use, sharing, adaptation, distribution and reproduction in any medium or format, as long as you give appropriate credit to the original author(s) and the source, provide a link to the Creative Commons licence, and indicate if changes were made. The images or other third party material in this article are included in the article's Creative Commons licence, unless indicated otherwise in a credit line to the material. If material is not included in the article's Creative Commons licence and your intended use is not permitted by statutory regulation or exceeds the permitted use, you will need to obtain permission directly from the copyright holder. To view a copy of this licence, visit http://creativecommons.org/licenses/by/4.0/.

Conclusion Digital speech-based assessments may have limited current utility for detecting FC alterations in at-risk individuals. Further validation using complementary methodological approaches, shorter intervals between fMRI and speech assessments, and testing in independent cohorts, are essential to establish their reliability and clinical relevance for monitoring brain network changes.

Keywords Functional MRI, Multicenter, Speech, Digital assessment, Alzheimer's disease spectrum

Background

As prevention-focused and combinatorial therapeutic strategies to address the pre-symptomatic stages of Alzheimer's disease (AD) are being developed, those with mild cognitive impairment (MCI), as well as cognitively normal individuals who might be at risk of developing AD, are increasingly taking part in clinical trials [1]. This trend underscores the need for easy-to-use and widely available tools for tracking cognition, where they might be used to identify risk in clinical care or targeted into clinical trials [2]. Digital cognitive tests for this purpose are a promising approach that is becoming more and more accepted, particularly in preclinical and prodromal AD research studies [3, 4]. These remote automated methods can both improve efficiency and reduce the burden on-site, whilst enabling the recruitment of participants from a broader and more diverse range of groups [4, 5].

Assessment based on verbal response is especially valuable because it can capture subtle linguistic and acoustic changes that often occur in early AD [6, 7]. Semantic Verbal Fluency (SVF) for testing executive function and semantic retrieval [8], and the Verbal Learning Task (VLT) for assessing episodic memory [9], are frequently used tasks for speech feature extraction. Speech features from these two tasks can identify subtle cognitive changes that usually remain unnoticed by global cognitive measures [10, 11]. Moreover, distinguishing subjective cognitive decline (SCD) from MCI/AD has become more accurate when speech features and task scores are combined [12, 13]. These features have also been related to traditional neuropsychological scores and established AD biomarkers, including amyloid beta (Aβ) and phosphorylated tau levels [14, 15]. Notably, it has recently been shown that cognitive composite scores that are exclusively computed from these speech features were correlated with standardized neuropsychological results, such as the validated speech-based cognitive (SB-C) scores [16]. It has also been reported that the SB-C scores were associated with longitudinal changes in cognition and brain atrophy [17]. But we are not yet sure whether these speech-derived indicators can signify other brain pathologies beyond volumetric alteration. Closing this gap could help clarify the extent to which speech-based tools can serve as a window into broader brain dysfunctions related to AD progression.

Of the various modalities, functional connectivity (FC) is a particularly good option for examination. Changed FC has also been considered a sensitive neuroimaging marker for early AD diagnosis, with the potential to be identified even before the onset of clinical cognitive deficits [18, 19]. Resting-state functional MRI (rs-fMRI), which does not require subjects to perform any tasks while scanning, is widely used to measure FC. Accordingly, this method is particularly appropriate for studies involving populations with cognitive impairments [20, 21]. By using rs-fMRI, researchers can investigate global FC at the network level to understand how different regions of the brain interact with one another. Research on AD has investigated several well-defined networks, including the default mode network (DMN), the executive control network (ECN), and the language network (LAN) [19, 22–26]. From all results, changes in the connectivity of the DMN have emerged as one of the most consistent findings in studies involving both AD and MCI groups [23, 27, 28]. This disruption in the DMN has also been associated with memory issues [23, 29, 30] and an increased risk of disease progression [31]. Research also showed that ECN connectivity alterations were correlated with executive dysfunction, manifested by abnormalities in the lateral prefrontal cortex and its connections with parietal and subcortical regions. Significant differences have been identified between individuals with MCI/AD and healthy people [23, 24, 26]. Changes in FC in the LAN have also been reported, showing links to semantic processing and connected speech deficits, with evidence showing that alterations in network-specific connectivity may support language performance in early phases of disease [25, 32].

Building on this rationale, the present study investigated how SB-C scores and key speech features associated with FC within related networks were affected in at-risk AD populations, including the DMN, ECN, and LAN. Our hypotheses were grounded in prior evidence linking specific cognitive abilities, as measured by speech-based tasks, to distinct neural networks. For this purpose, we examined (1) the associations between SB-C scores and connectivity patterns across these three networks; (2) the associations between SVF features and connectivity in the ECN and LAN; and (3) the associations between VLT delayed recall features and DMN connectivity. This network-specific approach aimed to deepen our understanding of how digital speech markers

correspond to potential underlying changes of the neural networks, providing evidence for their possible use as objective proxies for brain alterations and informing the development of sensitive, scalable tools for detecting cognitive decline risk.

Methods

Recruitment and sample

We used data from the German arm of the PROSPECT-AD study, a multicenter prospective initiative aimed at validating speech-based markers for the early detection and monitoring of AD [33]. The study design and protocol have been described in detail [33]. PROSPECT-AD integrates automated speech-based neurocognitive assessments into ongoing longitudinal cohorts, including DESCRIBE and DELCODE in Germany [34].

Participants aged 50 years or older were recruited from the DESCRIBE and DELCODE cohorts, representing a continuum of risk for developing AD dementia. Exclusion criteria were unstable medical conditions, major psychiatric disorders, or substance abuse. Of the 234 initially enrolled participants, 10 were excluded due to incomplete speech assessments. An additional group of participants was excluded due to the absence of qualified MRI scans, resulting in a final sample of 132 individuals. This sample comprised healthy controls (HC) and participants with SCD or MCI. The informed consent of all participants was obtained, and local ethics committees granted approval for the procedures.

Site clinicians determined clinical diagnoses based on structured clinical interviews, neuropsychological assessments, and established diagnostic criteria as follows. The HC group included individuals without cognitive complaints or objective impairment, as well as cognitively healthy first-degree relatives of AD patients. SCD was defined as persistent self-reported cognitive decline without objective impairment [35], while MCI was diagnosed according to the NIA criteria [36, 37].

Speech features collection, processing, and selection

Speech assessments were conducted remotely using the automated phonebot 'Mili' (ki:elements GmbH, Germany, https://ki-elements.de/mili-platform/). Participants were asked to complete six phone assessments over 15 months. The current analysis focused on data collected during the first call. Each speech assessment lasted approximately 15 min and included the following tasks: VLT (15-word, across 4 encoding trials), SVF (animal category, 1 min), a one-minute storytelling task describing a positive life event, and the delayed recall of the VLT at the end.

Speech recordings from the VLT and SVF tasks were processed using ki:elements' proprietary SIGMA speech analysis pipeline [38, 39]. This included German-optimized automatic speech recognition, transcription, voice analysis, and feature extraction. Based on speech features, the SB-C global score and three domain-specific SB-C subscores (executive function, learning and memory, and processing speed) were computed (Fig. 1).

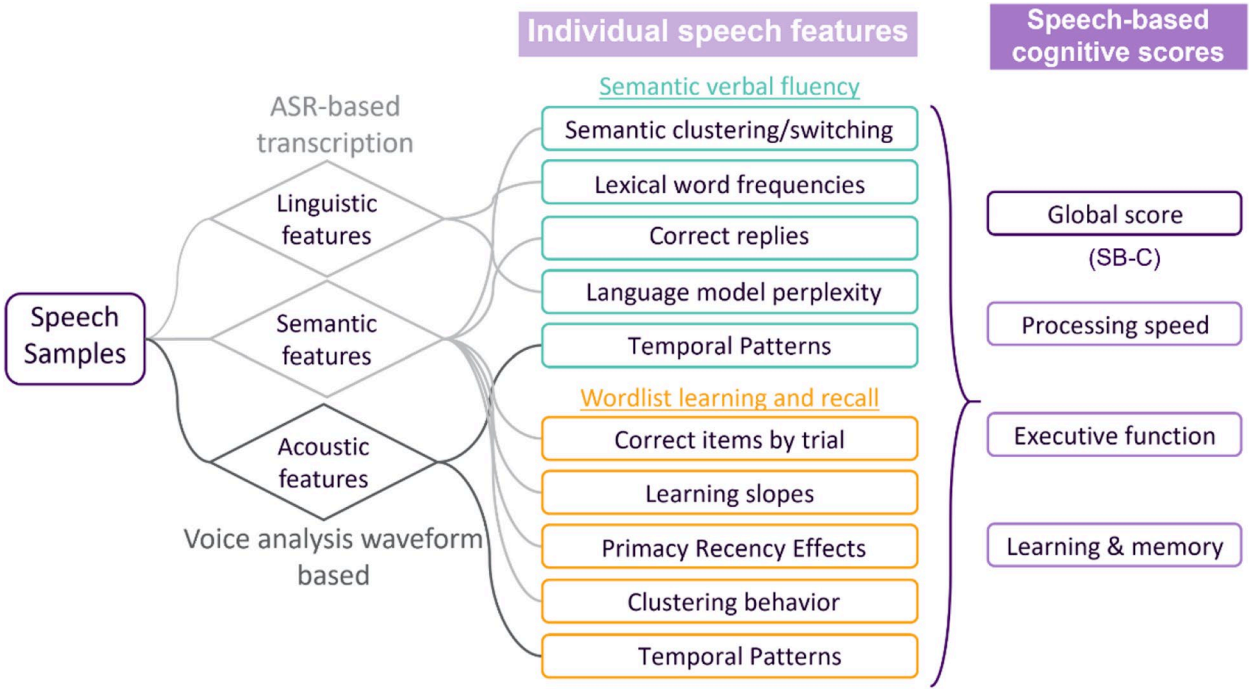

Fig. 1 Schematic representation of the processing steps involved in collecting and calculating the SB-C scores

Besides the SB-C global and subscores, we selected a hypothesis-driven subset of speech features based on their theoretical relevance to detect subtle cognitive changes sensitively. For the SVF task, we used correct replies (i.e., correct count) as a general measure, alongside lexical-semantic clustering/switching features including semantic cluster size and switch counts, which have established associations with semantic memory and executive function [11]. Word frequency was included because it relates to early word-finding difficulties and changes in word production in AD [40]. Temporal features, including temporal cluster size and switch counts, which complemented semantic features by measuring patterns of exploitation and exploration [42], were also included. For the VLT, we focused exclusively on delayed recall features, which comprised correct recall counts, word position-based measures (primacy, midlist, recency), and serial clustering size. This focus is supported by evidence that poor delayed recall performance is one of the early signs of episodic memory impairment and progression to AD [55]. Among the selected features, serial clustering size was chosen to capture sequential recall patterns linked to episodic memory organization [43]. Additionally, poorer recall of early list items during delayed recall, known as a diminished primacy effect, has been identified as a sensitive predictor of subsequent cognitive decline in AD [10]. All selected features, except primacy items, have also been identified among top speech recognition markers differentiating SCD from MCI/dementia [12, 13]. The full list of selected features and their descriptions is provided in the supplementary material (Table S1).

Imaging acquisition and processing

Imaging data were acquired using identical acquisition parameters and harmonized protocols from nine Siemens 3.0 Tesla MRI scanners (4 Verio, 1 Skyra, 3 Tim-Trio, and 1 Prisma system) at all study sites. To keep the data quality uniform, a semi-automated quality control process was implemented during the acquisition phase, with feedback provided to sites in case of protocol deviations. High-resolution T1-weighted structural MRI was obtained using a sagittal magnetization-prepared rapid gradient echo (MPRAGE) sequence with the following parameters: matrix size = 256 × 256, number of slices = 192, field of view = 256 × 256 mm, isotropic voxel size = 1 mm, repetition time = 2500 ms, echo time = 4.37 ms, flip angle = 7°, and parallel imaging acceleration factor = 2. Rs-fMRI data were collected using a T2*-weighted echo-planar imaging (EPI) sequence with the following parameters: matrix size = 64 × 64, 47 axial slices (thickness 3.5 mm, no gap) with interleaved acquisition, field of view = 224 × 224 × 165 mm, isotropic voxel size = 3.5 mm, repetition time = 2580 ms, echo time = 30 ms, flip angle = 80°, and parallel imaging acceleration factor = 2. A total of 180 EPI volumes were acquired over an 8-min scan.

There was no systematic approach to synchronize imaging and speech assessment because both were part of ongoing longitudinal studies. Therefore, for the purpose of minimizing the temporal mismatch, the closest MRI scan to a speech assessment was chosen for each subject.

Data processing was carried out using Data Processing Assistant for Resting-State fMRI Advanced (DPARSFA 5.3) [44] implemented in MATLAB R2020a (MathWorks, Natick, MA). The first 10 time points were discarded to allow for magnetic field stabilization and participant adaptation. Rs-fMRI data underwent slice-timing correction and realignment to the mean functional image to correct for head motion. During realignment, all functional images were resliced to an isotropic voxel size of 3 × 3 × 3 mm. The T1-weighted anatomical images were segmented into gray matter, white matter, and cerebrospinal fluid using the segmentation function within DPARSFA, which utilizes SPM12 (Statistical Parametric Mapping, Wellcome Trust Centre for Neuroimaging, London, UK, http://www.fil.ion.ucl.ac.uk/spm/), *New Segment* toolbox. Spatial normalization to Montreal Neurological Institute (MNI) space was performed using deformation fields generated by DARTEL (Diffeomorphic Anatomical Registration Through Exponentiated Lie Algebra) [45]. Residual head motion was evaluated by calculating the mean frame-wise displacement [46], with 0.5 mm being the cutoff for exclusion. After normalization, functional data were band-pass filtered (0.01–0.1 Hz) and smoothed using Gaussian kernels of varying full-width at half-maximum (FWHM) (see Sect. " Independent component analysis and dual regression" for details of smoothed kernels).

Independent component analysis and dual regression

We applied a single-group independent component analysis (ICA) by pooling all qualified resting-state scans across diagnostic groups to derive intrinsic connectivity networks that reflect a shared functional architecture across participants. This approach provided a common spatial reference for subsequent association analyses, ensuring that relationships between speech features and functional connectivity can be mapped consistently across individuals spanning the AD-risk spectrum. The resting-state FC (rsFC) maps were calculated using FSL (Version 5.0.9, FMRIB, Oxford, UK, http://www.fmrib.ox.ac.uk/fsl/) *melodic* toolbox, resulting in group-level ICA maps. As no standardized criteria exist for optimal smoothing kernels or ICA dimensionalities in the literature [47, 48], we systematically tested combinations of preprocessing parameters, including spatial smoothing

kernels of 6, 8, 10 mm, and ICA with 10, 20, 25, 30, and 40 components. The optimal combination was selected based on three criteria: (1) the spatial stability across runs, (2) the least inter-component correlations, and (3) the moderate-to-high spatial overlap with established functional templates. Of the different combinations we tested, the solution with an 8 mm smoothing kernel and 40-component ICA best met our criteria. Importantly, this configuration enabled the reliable identification of the LAN, which was not consistently detectable at lower ICA dimensionalities.

The generated independent components (ICs) were evaluated independently by two trained researchers and confirmed by experts to identify the three resting-state networks (RSNs) of interest, including DMN, ECN, and LAN. We used the *FSLcc* tool to measure correlations between ICs and established network templates [49, 50]. In addition, the ICs were visually inspected to select those covering key regions involved in each network, including the left inferior frontal gyrus and left posterior superior temporal gyrus for LAN, the posterior cingulate cortex (PCC) for DMN, and the medial prefrontal cortex for ECN. Identified ICs were also compared across multiple ICA configurations to assess the stability and consistency of the derived networks. For ICs showing spatial variability, we conducted sensitivity analyses to evaluate whether the ICA pooling strategy affected our primary results (Supplement 1). Subject-level rsFC z-maps were estimated using *dual regression* implemented in FSL, following ICA. This included (1) regressing the group-level spatial maps into each subject's 4D dataset to extract individual time courses, and (2) regressing these time courses back into the same dataset to obtain subject-level spatial maps for each RSN [51, 52]. We then performed a subsequent analysis to check whether these spatial maps were statistically different between diagnostic groups (Supplement 1, Table S5). Overall, the spatial topography of the DMN, ECN, and LAN did not differ significantly between diagnostic groups, confirming that the networks are representative of all participants.

For subsequent regression analyses, explicit masks for each RSN of interest were created by thresholding and binarizing the group-level ICs. DMN and ECN were thresholded at the top 10% of voxel intensities [23], while the LAN was thresholded using a T-value cutoff (peak $T > 5.0$) to achieve a better spatial specificity.

Statistical analysis

Statistical analyses were conducted using R version 4.4.2 [53], with functions from the *stats* package, and the non-parametric permutation-based tool *randomize* implemented in FSL. Group differences in demographic variables and speech features were assessed using one-way ANOVA with Tukey's honest significant difference (HSD) post-hoc tests. For variables that violated normality assumptions, Kruskal–Wallis tests were applied, and chi-squared tests were used for categorical variables. Statistical significance was set at $p < 0.05$.

Voxel-wise multiple regressions were performed using general linear models with 5,000 permutations. Speech features and SB-C scores were regressed on the rsFC z-maps hypothesized to be relevant. SVF word frequency was modeled to detect negative associations with rsFC, while all other speech features were modeled for positive associations. Covariates included age, sex, education, diagnosis, scan site, and the time interval between speech assessment and MRI acquisition to account for potential temporal mismatch.

To examine potential group differences in the associations between speech-derived measures and functional connectivity, we additionally fitted models including speech feature × diagnosis interaction terms within the primary ICA-based framework. Sensitivity analyses employing a complementary seed-to-voxel approach were conducted to validate the ICA-derived network definitions and replicate the across-group association results (see Supplement 2 for full details).

Statistical significance was determined using Threshold-Free Cluster Enhancement (TFCE) with family-wise error (FWE) correction at $p < 0.05$ [54]. When no clusters survived correction, a more liberal descriptive threshold of uncorrected $p < 0.01$ with a minimum cluster size of 20 voxels was applied. To ensure that identified effects reflected network-level connectivity patterns, significant voxel-wise results were mapped onto our predefined group-level RSN masks derived from ICA and visualized using *MRIcroGL* (https://www.nitrc.org/projects/mricrogl/.). A chord diagram was generated in R using the *circlize* package, illustrating the number of significant voxels and the strength of associations (T-values) between speech features and RSN regions.

Results

Demographic and speech characteristics

After excluding 3 participants for excessive head motion, the final sample included 129 individuals (32 HC, 72 SCD, 25 MCI; mean age = 73 years; 55% female; mean educatio$N$ = 15 years; mean time interval between speech assessment and MRI acquisitio$N$ = 1.4 years). Diagnostic groups did not differ significantly in age, education, or time interval between speech assessment and MRI acquisition, but differed in sex distribution ($\chi^2 = 7.12$, $p = 0.03$). Significant group differences were found across SB-C scores and subdomain scores, with post-hoc tests indicating lower performance in the MCI group. Several speech features, including SVF correct count, semantic cluster size, and VLT delayed recall, also differed significantly across groups (Table 1).

Table 1 Sample description of the dataset

		Overall	HC	SCD	MCI	Group difference
	Mean (SD)	**(*N* = 129)**	**(*N* = 32)**	**(*N* = 72)**	**(*N* = 25)**	***Post-hoc***
Demographic	**Age at scan**	72.8 (6.57)	73.4 (5.83)	72.3 (6.61)	73.7 (7.42)	$F(2, 126) = 0.51$, $p = 0.60$[a]
	Sex (f, %)	71 (55%)	24 (75%)	36 (50%)	11 (44%)	**$X^2(2) = 7.12$, $p = 0.03$[b]**
	Education (years)	14.9 (2.68)	14.8 (2.62)	15.1 (2.67)	14.3 (2.82)	$H(2) = 2.18$, $p = 0.337$[c]
	Number of scan sites	8	3	7	6	
	Time interval (years)	1.38 (2.22)	2.27 (2.98)	1.15 (1.89)	0.89 (1.69)	$H(2) = 1.53$, $p = 0.47$[c]
	MMSE score[d]	29.0 (1.41)	29.2 (1.26)	29.4 (0.98)	27.9 (2.01)	**$H(2) = 15.05$, $p < 0.001$[c]**
						MCI-HC*
						MCI-SCD***
SB-C global	**Global cognition score**	0.67 (0.25)	0.74 (0.27)	0.70 (0.19)	0.49 (0.28)	**$F(2, 126) = 9.86$, $p < 0.001$[a]**
						MCI-HC***
						MCI-SCD***
SB-C subdomain	**Executive score**	0.50 (0.22)	0.53 (0.22)	0.53 (0.20)	0.38 (0.23)	**$F(2, 126) = 5.38$, $p < 0.01$[a]**
						MCI-HC*
						MCI-SCD**
	Memory score	0.57 (0.20)	0.61 (0.21)	0.59 (0.16)	0.44 (0.23)	**$H(2) = 10.61$, $p < 0.01$[c]**
						MCI-HC**
						MCI-SCD*
	Processing speed score	0.74 (0.31)	0.83 (0.34)	0.77 (0.24)	0.57 (0.36)	**$F(2, 126) = 6.00$, $p < 0.01$[a]**
						MCI-HC**
						MCI-SCD*
SVF	**Correct count**	20.3 (6.80)	20.4 (6.51)	21.9 (6.10)	15.7 (7.21)	**$F(2, 126) = 8.63$, $p < 0.001$[a]**
						MCI-HC*
						MCI-SCD***
	Word frequency	3.63 (0.25)	3.62 (0.28)	3.59 (0.20)	3.76 (0.28)	**$F(2, 126) = 4.66$, $p = 0.01$[a]**
						MCI-SCD**
	Semantic cluster size	3.54 (1.29)	3.41 (1.14)	3.84 (1.33)	2.86 (1.07)	**$H(2) = 13.68$, $p < 0.001$[c]**
						MCI-SCD***
	Semantic cluster switches	5.37 (2.02)	5.63 (1.84)	5.35 (2.14)	5.12 (1.90)	$H(2) = 0.84$, $p = 0.66$[c]
	Temporal cluster size	4.19 (1.98)	4.63 (2.44)	4.10 (1.64)	3.89 (2.20)	$H(2) = 3.21$, $p = 0.20$[c]
	Temporal cluster switches	4.60 (2.07)	4.28 (1.85)	4.99 (2.05)	3.92 (2.20)	**$F(2, 126) = 3.09$, $p = 0.049$[a]**
VLT delayed recall	**Correct count**	10.3 (3.44)	10.9 (2.88)	11.2 (2.64)	7.08 (4.27)	**$H(2) = 19.53$, $p < 0.001$[c]**
						MCI-HC**
						MCI-SCD***
	Midlist items	4.91 (1.81)	5.22 (1.68)	5.29 (1.45)	3.44 (2.18)	**$H(2) = 15.07$, $p < 0.001$[c]**
						MCI-HC**
						MCI-SCD***
	Primacy items	2.74 (1.19)	2.78 (1.13)	3.01 (0.942)	1.92 (1.53)	**$H(2) = 10.35$, $p < 0.01$[c]**
						MCI-SCD**
	Recency items	2.67 (1.16)	2.94 (1.05)	2.89 (1.00)	1.72 (1.28)	**$H(2) = 17.37$, $p < 0.001$[c]**
						MCI-HC***
						MCI-SCD***
	Serial clusters	3.26 (2.40)	3.34 (2.59)	3.43 (2.17)	2.68 (2.75)	$H(2) = 4.10$, $p = 0.13$[c]

[a]Univariate ANOVA

[b]Chi-square test

[c]Kruskal–Wallis H test

[d]Mini–Mental State Examination

*$p < 0.05$, **$p < 0.01$, ***$p < 0.001$, significant results are marked in bold.

Group-level ICA-derived resting-state networks

Our ICA-derived RSNs showed moderate to strong spatial correlations with network templates from Shirer et al. [49], with correlation values of 0.77 for the DMN, 0.53 for the ECN, and 0.48 for the LAN. All selected components exhibited substantial overlap with key regions relevant to their respective networks.

The DMN derived from ICA at the group-level was composed of bilateral regions and the spatial map was largely symmetric (Fig. 2A). Key regions included the precuneus, superior frontal gyrus, posterior orbitofrontal cortex, and ventral lateral thalamus. In the left hemisphere, clusters were observed in the cerebellum (Lobule 9 and Crus II) and inferior frontal gyrus (Table S2). The ECN showed strong connectivity in the left inferior parietal lobule and inferior temporal gyrus, with additional clusters in the right middle frontal gyrus and thalamus (Table S2, Fig. 2B). The LAN was primarily left-lateralized, with the largest cluster located in the left middle temporal gyrus. Additional clusters were found in the left

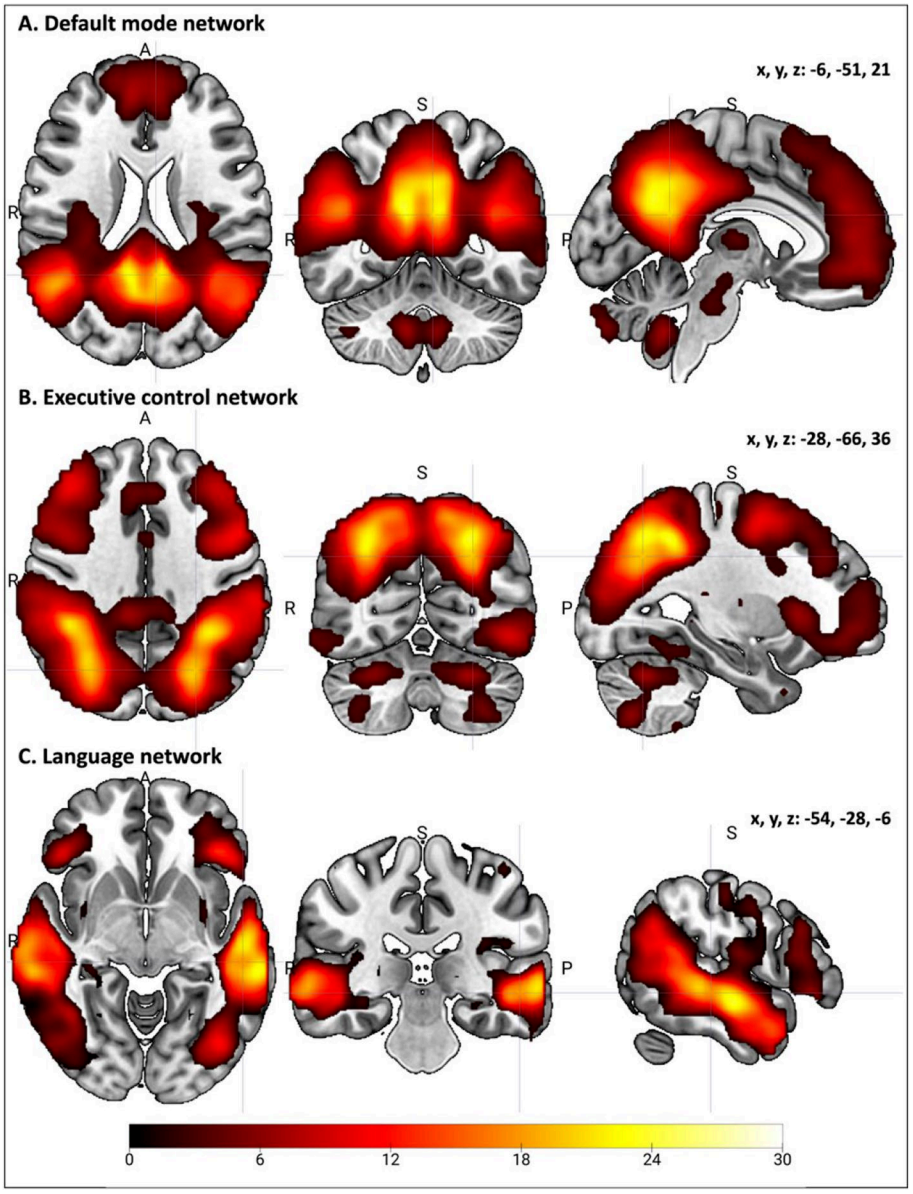

Fig. 2 Group-level ICA-derived resting-state networks (RSNs). Spatial maps of the (**A**) default mode network (DMN), (**B**) executive control network (ECN), and (**C**) language network (LAN) identified using a forty-component ICA decomposition with an 8 mm smoothing kernel. DMN and ECN maps were visualized by displaying the top 10% of voxel intensities from the group-level component maps, whereas the LAN was thresholded at a peak T-value > 5, highlighting the most strongly contributing regions. These thresholded maps were also used to generate binarized masks for subsequent regression analyses. All results are shown in MNI space over a standard anatomical template. Images are shown in radiological convention (left = right hemisphere). The color scale represents *t*-values.

precuneus and cerebellum (Lobule 8), and in the right cerebellum (Lobule 9) (Table S2, Fig. 2C).

Sensitivity analyses across multiple ICA configurations indicated that the DMN and ECN were highly stable. Group-level components captured most voxels from individual groups, with strong spatial correspondence across configurations (DMN Dice 0.74 ± 0.07, ECN Dice 0.75 ± 0.05; spatial correlation DMN 0.90 ± 0.06, ECN 0.88 ± 0.13; Table S3). The LAN was more variable (Dice 0.45 ± 0.07, spatial correlation 0.35 ± 0.22; Table S3), yet core regions such as left inferior frontal gyrus and left posterior superior temporal gyrus were consistently identified (Fig. S1).

Network-specific resting-state connectivity associated with speech-based cognitive performance and features

Of all the associations examined, the only statistically significant finding after correction was a positive association between LAN connectivity and SVF temporal cluster switching. This effect was localized to the left middle temporal gyrus (12 voxels, mean T = 3.86, peak T = 4.08; peak MNI coordinates: – 57, – 51, 12). Sensitivity analyses using an alternative ICA configuration confirmed that this association, along with other LAN-speech associations reported below, remained consistent across ICA template strategies (Table S4). To support interpretation, exploratory results using a liberal threshold ($p < 0.01$ uncorrected, cluster size ≥ 20 voxels) are also reported (Fig. 3, Table 2). All analyses were restricted to the group-level RSN masks.

Cognitive composite scores associated with connectivity in DMN, ECN, and LAN

No significant associations were observed between SB-C scores, either global or domain-specific, and connectivity in any of the three RSNs.

SVF features associated with connectivity in ECN and LAN

At an uncorrected threshold, SVF correct counts were associated with LAN connectivity in the left inferior temporal gyrus (Fig. 3, Table 2). SVF semantic cluster size showed a wide range of associations with ECN connectivity, involving the bilateral middle frontal gyri, left middle temporal gyrus, cerebellar regions, right inferior frontal and precentral areas, bilateral precuneus, and right superior and postcentral frontal cortices (Fig. 3,

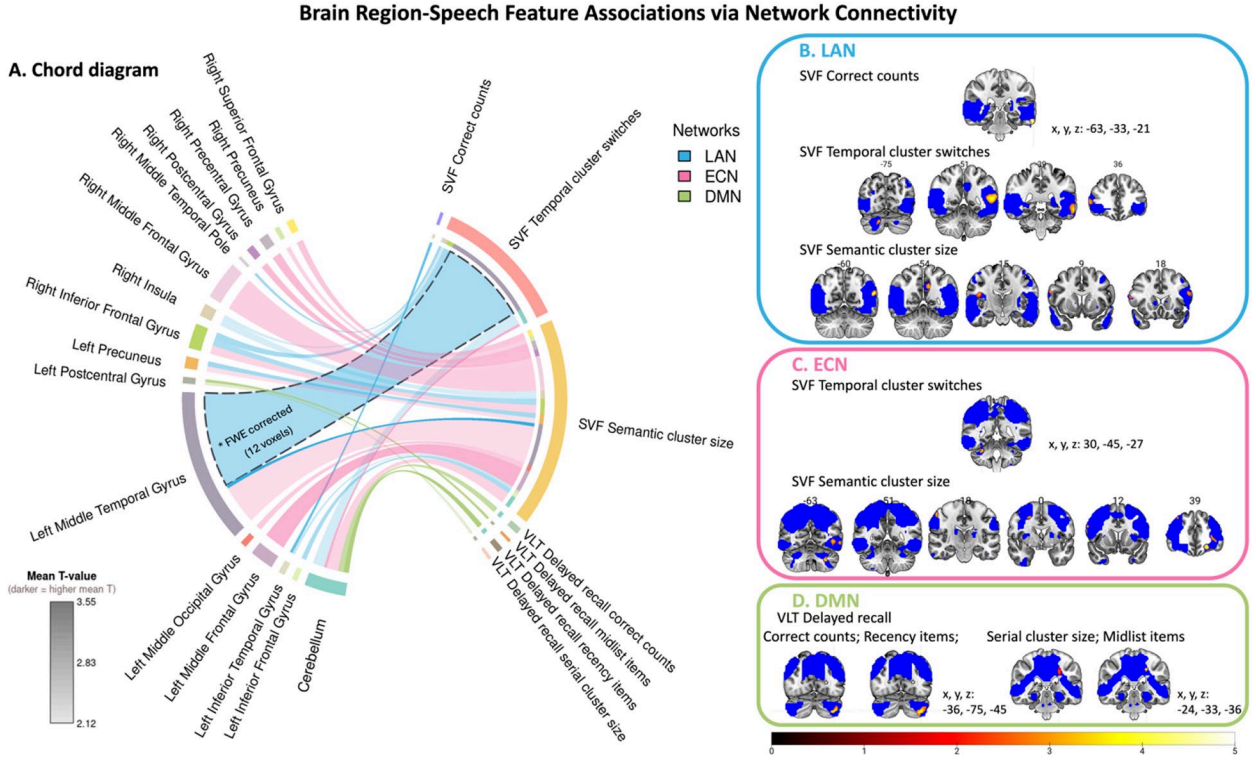

Fig. 3 Brain Region-Speech Feature Relationships via Network Connectivity. Associations are shown at an uncorrected p < 0.01 with a minimum cluster size of 20 voxels. **(A)** Chord diagram illustrating associations between speech features and FC of brain regions within RSNs. Line thickness represents the number of significant voxels mapped to each network-level association, line transparency reflects the mean T-value across voxels (less transparent indicates stronger effects), and line color denotes the corresponding network. **(B–D)** Brain regions in which FC was associated with different speech features, mapped onto group-level RSN masks. Blue voxels indicate RSNs, and warm-colored voxels (T-value color scale) indicate regions showing significant associations. Statistical maps are overlaid on the MNI template brain. All models were adjusted for age, sex, education, diagnosis, scan site, and the time interval between speech assessment and MRI. Images are displayed in radiological convention (left = right hemisphere).

Table 2 Brain regions showing significant associations between resting-state network connectivity and digital speech features

Digital speech features		network	Cluster size (voxels)	mean T	peak MNI Coordinates			peak T	Side	Anatomical location
SVF	Correct counts	LAN	23	3.08	−66	−33	−27	3.90	L	Inferior Temporal Gyrus
	Semantic cluster size	ECN	92	2.30	−30	−63	−39	3.81	L	Cerebellum Crus 1
			304	2.20	−42	−57	0	3.53	L	Middle Temporal Gyrus
			168	2.74	−24	39	−12	4.28	L	Middle Frontal Gyrus, part 2
			267	2.35	36	36	48	3.59	R	Middle Frontal Gyrus, part 2
			44	2.40	−24	−57	33	3.49	L	Middle Occipital Gyrus
			66	2.28	60	12	27	3.29	R	Opercular Inferior Frontal Gyrus
			35	2.30	18	−51	33	3.19	R	Precuneus
			54	2.46	21	0	45	3.49	R	Superior Frontal Gyrus, part 2
			42	2.15	0	−75	48	2.94	L	Precuneus
			53	2.60	54	−18	54	3.65	R	Postcentral Gyrus
			70	2.61	45	−9	54	3.59	R	Precentral Gyrus
		LAN	22	2.23	−57	−27	−18	2.75	L	Inferior Temporal Gyrus
			63	2.12	45	−15	21	3.29	R	Insula
			38	2.49	−54	18	21	3.32	L	Inferior Frontal Gyrus, triangular part
			51	2.47	57	9	24	3.94	R	Opercular Inferior Frontal Gyrus
			27	3.55	−57	−60	21	4.19	L	Middle Temporal Gyrus
			39	2.57	−12	−54	36	3.43	L	Precuneus
	Temporal cluster switches	ECN	21	2.77	30	−45	−27	3.38	R	Cerebellum Lobule 6
		LAN	94	2.14	12	−75	−33	3.18	R	Cerebellum Crus 2
			733	**2.52**	**−57**	**−51**	**12**	**4.08**	**L**	**Middle Temporal Gyrus ***
			21	2.58	57	12	−21	2.95	R	Middle Temporal Pole
			55	2.53	57	36	6	3.39	R	Inferior Frontal Gyrus, triangular part
			25	2.14	33	−9	9	3.05	R	Insula
VLT delayed recall	Correct counts	DMN	45	2.91	−36	−75	−45	4.08	L	Cerebellum Crus 2
	Midlist items	DMN	21	3.22	−24	−33	39	3.89	L	Postcentral Gyrus
	Recency items	DMN	42	3.36	−36	−75	−45	4.60	L	Cerebellum Crus 2
	Serial cluster size	DMN	24	2.32	−24	−33	36	2.74	L	Postcentral Gyrus

Uncorrected threshold of $p < .01$, with cluster size ≥ 20 voxels

*12 voxels in this cluster survived correction (mean T = 3.86, peak T = 4.08, $p_{FWE} < 0.05$), significant results are marked in bold.

Table 2). Within the LAN, semantic cluster size was associated with connectivity in the left inferior and middle temporal gyri, bilateral inferior frontal gyrus, right insula, and left precuneus (Fig. 3, Table 2). Temporal cluster switching during SVF was associated with connectivity in the right cerebellum (Crus 2), left middle temporal gyrus, right middle temporal pole, right inferior frontal gyrus (triangular part), and right insular regions within the LAN (Fig. 3, Table 2), as well as the right cerebellar lobule VI within the ECN (Fig. 3, Table 2).

VLT delayed recall features associated with connectivity within DMN

Within the DMN, VLT delayed recall correct counts and recency items were associated with connectivity in the left cerebellar Crus II (Fig. 3, Table 2). Serial cluster size and midlist items were associated with connectivity in the left postcentral cortex (Fig. 3, Table 2).

Complementary analyses of speech-functional connectivity associations

Models including speech feature × diagnosis interaction terms revealed limited evidence for group-specific associations. While some voxel-wise interactions survived TFCE correction, primarily within LAN-related regions, the majority of these significant voxels fell outside our predefined IC network masks. The only interaction effect that localized within our RSNs was confined to 3 voxels in the ECN. These findings suggest that the associations between speech-derived measures and functional connectivity do not differ substantially across diagnostic groups at the network level (Table S6).

Seed-to-voxel analyses, which complement the ICA-based network findings, are provided in the Supplementary Materials. The spatial patterns of the seed-defined RSNs largely aligned with ICs, supporting the consistency of network identification across methods (Fig. S2).

However, associations with digital speech-based metrics showed partial overlap, indicating method-dependent variability in regression sensitivity. Importantly, these seed-based associations were exploratory, identified using an uncorrected threshold ($p < 0.01$, cluster size ≥ 20 voxels, Table S7, Fig. S2).

Discussion

This study investigated associations between digital speech–derived cognitive composite scores, task-specific speech features, and rsFC within the DMN, ECN, and LAN across 129 individuals from cognitively healthy to MCI in the German PROSPECT-AD study. We hypothesized that both SB-C scores and speech features would be sensitive to subtle network-specific FC alterations in at-risk populations.

Primary finding: temporal cluster switching and FC in LAN

The significant result was that stronger LAN connectivity was associated with greater temporal cluster switching during SVF (TFCE-based FWE $p < 0.05$), suggesting more dynamic lexical access. This association was mostly observed in the left middle temporal gyrus, a region that has been implicated both in goal-directed and automatic semantic processes, as well as in controlled semantic retrieval [55]. These cognitive processes align with what the temporal switching feature captures: how verbal responses are arranged over time and the flexible retrieval strategies used during the task. Previous analyses combining temporal and semantic features have shown that these verbal patterns tend to decline in individuals with MCI and AD, even when semantic knowledge remains relatively preserved [41]. Our results are consistent with this theoretical relationship, indicating that temporal speech dynamics should be given priority in future research as a promising speech indicator of early LAN changes. However, the modest effect size and limited spatial extent require cautious interpretation. Replication in independent samples will be essential to confirm whether temporal cluster switching can reliably track LAN integrity among at-risk populations of AD.

Absence of associations with SB-C scores

Our ICA-based rsFC analyses did not find any significant association with global or domain-specific SB-C scores. Composite cognitive measures tend to have greater reliability and sensitivity than individual test scores in particular cognitive domains. They are therefore recommended for identifying subtle cognitive changes in at-risk groups [56, 57]. Additionally, common composites such as the Cognitive Function Composite (CFC) are less affected by practice effects, which makes them a suitable endpoint in longitudinal studies or clinical trials [2, 57]. Despite these theoretical advantages, the absence of significant findings contrasts with previous studies linking cognitive composites to rsFC in MCI [30, 58] and with our own prior PROSPECT-AD findings showing SB-C associations with clinical measures and brain atrophy across diagnostic groups [16, 17].

One explanation could be the intended purpose of SB-C scores. SB-C scores have been designed for assessing general cognitive performance across executive function, memory, and processing speed [39]. While our objective was to examine the broader clinical potential of SB-C scores by linking them to underlying brain FC alterations, this inclusivity may fundamentally limit their sensitivity to network-specific FC changes, highlighting a general challenge of using composite scores to detect subtle neuropathology. One real-world example is the Preclinical Alzheimer's Cognitive Composite (PACC). Although PACC is widely used to track cognitive decline in preclinical AD [59], studies have indicated varying degrees of reliability in detecting baseline Aβ status [60, 61] . This observation underscores that general composite scores have limitations in certain contexts. Also, the subtle nature of network FC alterations at very early stages of AD may exceed the detection threshold of broad composite measures. This suggests that composite cognitive measures might require support from complementary approaches to capture network-specific brain alterations more sensitively.

Rather than relying solely on composite scores that aggregate across cognitive domains, future research could use data-driven techniques such as principal component analysis of speech features to apply more analytical strategies focused on the speech-FC connection. By utilizing both the clinical interpretability of domain-level scores and the discovery potential of unsupervised methods, this dual strategy could potentially uncover speech features that are more closely linked to underlying FC patterns.

Methodological considerations: ICA approach and network identification

Initial analyses (uncorrected $p < 0.01$) suggested additional connections between SVF features and ECN/LAN connectivity, and between VLT delayed recall features and DMN connectivity. We therefore systematically evaluated whether our ICA approach introduced bias that could account for the absence of significant associations between rsFC and SB-C scores, as well as the largely exploratory nature of the rsFC-speech findings. We raised this concern because heterogeneity in automated RSN derivation remains a recognized methodological challenge, as analytical parameter variations can substantially alter network topology and localization [47, 48].

Spatial maps of the DMN and ECN were highly consistent across all ICA pooling configurations, with balanced

contributions from diagnostic groups. This ruled out meaningful bias from our SCD-dominant sample (56% of participants). In contrast, LAN identification proved more challenging. Across all configurations, 40 components were required to isolate a single network covering all key language-related regions, with no clear hemispheric subdivision. This contrasts with previous work using substantially larger samples, which identified left- and right-lateralized language-related networks applying only 20 components [50]. The LANs we identified also showed greater spatial variability across ICA configurations.

This pattern is in line with heterogeneous LAN alterations in the AD spectrum reported previously, including reduced connectivity within semantic control networks in mild AD [32] and increased LAN activations in MCI [62]. However, when we examined individual spatial FC maps, we did not find significant differences between diagnostic groups. This may reflect the early-stage expression of LAN alterations at the pre-dementia stages represented in our sample. This interpretation is consistent with prior DELCODE findings where LAN showed only chance-level classification performance in SCD and MCI, with group differences emerging only under liberal thresholds [23, 26].

When we reran analyses using a different LAN template, LAN rsFC-speech associations remained highly consistent, indicating that the ICA pooling approach did not materially influence our results. Instead, this pattern is more plausibly attributable to the small effect sizes characteristic of rsFC–speech associations in heterogeneous early-stage AD populations, consistent with large-scale brain-wide association studies showing that relationships between complex behavioral phenotypes and FC are much weaker than previously assumed, requiring sample sizes in the thousands for reliable detection [63]. Given our present sample size, limited statistical power rather than methodological bias or absent brain-behavior relationships likely accounts for the observed results.

Complementary seed-based analyses

We performed seed-based analyses to supplement our ICA results. The reliability of our ICA-derived RSN characterization was supported by consistent network identification between the two methods. Seed analyses also revealed associations between speech features and FC at the exploratory level. However, we do not recommend relying primarily on seed-based approaches or applying them as an exclusive analytical strategy. Meta-analyses have demonstrated that even minor changes in seed selection within the DMN can produce substantial variability in results, raising questions about the reliability of such methods [64]. Employing multiple analytical strategies may therefore yield complementary insights. Replication in independent populations, in addition to testing alternative implementations of analytic approaches, may enable future studies to reach credible and generalizable results while avoiding spurious associations.

Study strengths and limitations

While most remote cognitive assessment research has focused on group classification, cognitive associations, or amyloid burden correlations, we extended this by exploring links between SB-C scores, speech features, and brain functional connectivity to better understand their neural correlates. This hypothesis-generating study provides important methodological and conceptual insights for future research, but it also has limitations.

The one-year average interval between rs-fMRI and speech assessments is a crucial limitation. Although this has been statistically controlled, it may still add variability that limits precision. This limitation cannot be addressed within the current dataset, as data collection is already complete. However, it will be investigated in forthcoming longitudinal analyses that focus on associations between FC and speech changes over time. Another limitation of our study could also be that the methodologies that were focused on global FC may have potentially missed local connectivity. Hence, our findings might be complemented by using local connectivity metrics such as amplitude of low-frequency fluctuations (ALFF) or regional homogeneity (ReHo).

Conclusions

This study provides proof-of-concept that specific speech features, particularly temporal dynamics during SVF, show detectable associations with FC in LAN, even in early-stage populations spanning from cognitively healthy individuals to MCI. However, the effects are modest in size and limited in spatial extent, requiring replication before clinical application. Notably, SB-C scores did not show sufficient sensitivity to capture network-specific brain FC changes in our cohort, although they remain useful for tracking brain volumetric changes and general cognitive decline.

Future studies should use longitudinal designs that track rsFC-speech associations over time, significantly increase sample sizes to achieve an adequate statistical power, and harmonize data collection procedures across research sites while validating findings in diverse cohorts across different clinical stages and sociodemographic backgrounds in order to advance the development of speech-based digital tools for identifying and monitoring brain function alterations in populations at-risk of AD.

Abbreviations

AD	Alzheimer's disease
MCI	Mild cognitive impairment
SVF	Semantic Verbal Fluency
VLT	Verbal Learning Task
SCD	Subjective cognitive decline
Aβ	Amyloid beta
SB-C score	Speech-based cognitive score
FC	Functional connectivity
rs-fMRI	Resting-state functional MRI
DMN	Default mode network
ECN	Executive control network
LAN	Language network
HC	Healthy controls
rsFC	Resting-state functional connectivity
ICA	Independent component analysis
IC	Independent component
RSN	Resting-state network
TFCE	Threshold-Free Cluster Enhancement
FWE	Family-wise error

Supplementary Information

The online version contains supplementary material available at https://doi.org/10.1186/s13195-026-01993-x.

Supplementary Material 1.

Acknowledgements

We wish to acknowledge the support given to young researchers from the European Union's HORIZON-MSCA Doctoral Networks and funding from the Alzheimer's Drug Discovery Foundation for this study. We thank ki:elements for their AI-based software development and speech data collection efforts. Grateful acknowledgments are extended to DZNE and all PROSPECT-AD sites, as well as the DELCODE and DESCRIBE teams, for their contributions to the recruitment and clinical assessment of participants, the neurocognitive and MRI data collection, and the quality control. Thanks are due to the clinical and administrative teams at Rostock University Medical Center and the Rostock site of the DZNE for their support. We thank our study's co-authors for their work on the study design, project coordination, data curation, and manuscript writing. Most importantly, we thank the study participants for their time and effort in the PROSPECT-AD study.

Authors' contributions

Qingyue Li (Conceptualization; Methodology; Formal analysis; Visualization; Writing—Original Draft; Writing—Review & Editing), Zampeta-Sofia Alexopoulou (Formal analysis; Writing—Review & Editing), Martin Dyrba (Methodology; Writing—Review & Editing), Elisa Mallick (Software; Methodology; Investigation; Data Curation), Johannes Tröger (Software; Writing—Review & Editing), Eike Spruth (Data Curation; Investigation; Writing—Review & Editing), Slawek Altenstein (Data Curation; Investigation; Writing—Review & Editing), Claudia Bartels (Data Curation; Investigation; Writing—Review & Editing), Wenzel Glanz (Data Curation; Investigation; Writing—Review & Editing), Enise I. Incesoy (Data Curation; Investigation; Writing—Review & Editing), Michaela Butryn (Data Curation; Investigation; Writing—Review & Editing), Ingo Kilimann (Data Curation; Investigation; Writing—Review & Editing), Sebastian Sodenkamp (Data Curation; Investigation; Writing—Review & Editing), Franziska Maier (Data Curation; Investigation; Writing—Review & Editing), Ayda Rostamzadeh (Data Curation; Investigation; Writing—Review & Editing), Antje Osterrath (Data Curation; Investigation; Writing—Review & Editing), Josef Priller (Data Curation; Investigation; Writing—Review & Editing), Anja Schneider (Data Curation; Investigation; Writing—Review & Editing), Jens Wiltfang (Data Curation; Investigation; Writing—Review & Editing), Christoph Laske (Data Curation; Investigation; Writing—Review & Editing), Björn Falkenburger (Data Curation; Investigation; Writing—Review & Editing), Michael Wagner (Data Curation; Investigation; Writing—Review & Editing), Emrah Duezel (Data Curation; Investigation; Writing—Review & Editing), Annika Spottke (Data Curation; Investigation; Writing—Review & Editing), Gabor C. Petzold (Data Curation; Investigation; Writing—Review & Editing), Frank Jessen (Data Curation; Writing—Review & Editing), Alexandra König (Software; Conceptualization; Writing—Review & Editing), Stefanie Köhler (Project Administration; Data Curation; Writing—Review & Editing), Stefan Teipel (Conceptualization; Supervision; Investigation; Methodology; Writing—Review & Editing).

Funding

Open Access funding enabled and organized by Projekt DEAL. Qingyue Li and Zampeta-Sofia Alexopoulou receive funding from the European Union's HORIZON-MSCA Doctoral Networks 2021 program under grant agreement No 101071485. The PROSPECT-AD study is partially funded by the Alzheimer's Drug Discovery Foundation Diagnostic Accelerator program (ADDF). The funders of this study had no role in study design, data collection, data analysis, data interpretation, or writing the report.

Data availability

The dataset(s) supporting the conclusions of this article are not publicly available due to institutional policy, but are available from the corresponding author on reasonable request.

Declarations

Ethics approval and consent to participate

All data collection adhered to ethical standards for medical research involving human participants, following the Declaration of Helsinki and the European General Data Protection Regulation. The German PROSPECT-AD study received approval from local institutional review boards: University Hospital Bonn (291/22), Ethics Committee of the Technical University of Dresden (BO-EK-263062022), University Medical Center Goettingen (27/9/22), University of Cologne Faculty of Medicine (22–1284), University Hospital Magdeburg Medical Faculty (80/22), University Medical Center Rostock (A2021-0256), and University Hospital Tuebingen (551/2022BO2). For Charité Universitätsmedizin Berlin, no separate approval was required, as it relied on the one from Rostock as the lead site.

All participants provided written informed consent for speech data collection.

Consent for publication

Not applicable.

Competing interests

Martin Dyrba has received research funding from the Deutsche Forschungsgemeinschaft and lecture fees from Europäische Fernhochschule Hamburg GmbH. Alexandra König, Elisa Mallick, and Johannes Tröger are employed by the company ki:elements, which developed the application for the automatic phone assessment and calculated the speech biomarkers. Claudia Bartels received funding from the German Alzheimer's Association and lecture fees from Lilly, Boehringer Ingelheim, Novo Nordisk, and Eisai. Michaela Butryn has received lecture fees from Neuraxpharm. Ingo Kilimann has received an unrestricted research grant from Lilly Germany. Franziska Maier participated in scientific advisory boards of Lilly and Johnson & Johnson and received lecture fees from Novo Nordisk. Ayda Rostamzadeh received lecture fees from Eisai and Lilly. Jens Wiltfang has received funding from the BMBF, consulting fees from Immunogenetics, Noselab, Roboscreen, and lecture fees from Beijing Yibai Science and Technology Ltd., Gloryren, Janssen Cilag, Pfizer, Med Update GmbH, Roche Pharma, and Lilly. Jens Wiltfang participated on a Data Safety Monitoring Board or Advisory Board of Biogen, Abbott, Boehringer Ingelheim, Lilly, MSD Sharp & Dohme, and Roche. Björn Falkenburger has received advisory and consultancy honoraria from AbbVie, Bial, and is an investigator on studies funded by AbbVie, Bial, Biogen, CHDI, Denali, DFG, MJFF, Takeda, Teva, and UCB. Stefanie Köhler has received funding from the Alzheimer Drug Discovery Foundation and Lilly Deutschland GmbH, as well as lecture fees from Eisai. Stefan Teipel participated in scientific advisory boards of Roche Pharma AG, Biogen, Lilly, and Eisai, and received lecture fees from Lilly and Eisai. The other authors declared no potential conflicts of interest with respect to the research, authorship, and/or publication of this article.

Author details

[1]Department of Psychosomatic Medicine, Rostock University Medical Center, Gehlsheimer Str. 20, Rostock 18147, Germany
[2]Cognition-Behavior-Technology Lab (CoBtek), Université Côte d'Azur, Nice, France

[3]German Center for Neurodegenerative Diseases (DZNE), Rostock, Germany
[4]ki:Elements GmbH, Saarbrücken, Germany
[5]German Center for Neurodegenerative Diseases (DZNE), Berlin, Germany
[6]Department of Psychiatry and Psychotherapy, Charité, Berlin, Germany
[7]Department of Psychiatry and Psychotherapy, University Medical Center Göttingen, University of Göttingen, Göttingen, Germany
[8]German Center for Neurodegenerative Diseases (DZNE), Magdeburg, Germany
[9]Institute of Cognitive Neurology and Dementia Research (IKND), Otto-Von-Guericke University, Magdeburg, Germany
[10]German Center for Neurodegenerative Diseases (DZNE), Tübingen, Germany
[11]Department of Psychiatry and Psychotherapy, University of Tübingen, Tübingen, Germany
[12]Department of Psychiatry, Medical Faculty, University of Cologne, Cologne, Germany
[13]German Center for Neurodegenerative Diseases (DZNE), Dresden, Germany
[14]Department of Neurology, Carl Gustav Carus, Tec, University Hospital, hnische Universität Dresden, Dresden, Germany
[15]University of Edinburgh and UK DRI, Edinburgh, UK
[16]Department of Psychiatry and Psychotherapy, School of Medicine and Health, Technical University of Munich, and German Center for Mental Health (DZPG), Munich, Germany
[17]German Center for Neurodegenerative Diseases (DZNE), Bonn, Germany
[18]Clinic of Old Age Psychiatry and Cognitive Disorders, University Hospital Bonn and University of Bonn, Bonn, Germany
[19]German Center for Neurodegenerative Diseases (DZNE), Göttingen, Germany
[20]Department of Medical Sciences, Neurosciences and Signaling Group, Institute of Biomedicine (iBiMED), University of Aveiro, Aveiro, Portugal
[21]Clinic for Parkinson's, Sleep and Movement Disorders, Centre for Neurology, University Hospital Bonn, Bonn, Germany
[22]Department of Vascular Neurology, University Hospital Bonn, Bonn, Germany
[23]Excellence Cluster On Cellular Stress Responses in Aging-Associated Diseases (CECAD), University of Cologne, Cologne, Germany
[24]Centre Hospitalier Et Universitaire, Clinique Gériatrique du Cerveau Et du Mouvement, Centre Mémoire de Ressources Et de Recherche, Université Côte d'Azur, Nice, France

Received: 20 October 2025 / Accepted: 15 February 2026
Published online: 24 February 2026

References

1. Cummings JL, Zhou Y, Lee G, Zhong K, Fonseca J, Leisgang-Osse AM, et al. Alzheimer's disease drug development pipeline: 2025. Alzheimers Dement Transl Res Clin Interv. 2025;11(2).
2. Cohen S, Cummings J, Knox S, Potashman M, Harrison J. Clinical trial endpoints and their clinical meaningfulness in early stages of Alzheimer's disease. J Prev Alzheimers Dis. 2022;9(3):507–22.
3. Öhman F, Hassenstab J, Berron D, Schöll M, Papp KV. Current advances in digital cognitive assessment for preclinical Alzheimer's disease. Alzheimers Dement Diagn Assess Dis Monit. 2021;13(1).
4. Polk SE, Öhman F, Hassenstab J, König A, Papp KV, Schöll M, et al. A scoping review of remote and unsupervised digital cognitive assessments in preclinical Alzheimer's disease. Npj Digit Med. 2025;8(1).
5. Sabbagh MN, Lue LF, Fayard D, Shi J. Increasing precision of clinical diagnosis of Alzheimer's disease using a combined algorithm incorporating clinical and novel biomarker data. Neurol Ther. 2017;6(S1):83–95.
6. Taler V, Phillips NA. Language performance in Alzheimer's disease and mild cognitive impairment: a comparative review. J Clin Exp Neuropsychol. 2008;30(5):501–56.
7. Vigo I, Coelho L, Reis S. Speech- and language-based classification of Alzheimer's disease: a systematic review. Bioengineering. 2022;9(1):27.
8. Aita SL, Beach JD, Taylor SE, Borgogna NC, Harrell MN, Hill BD. Executive, language, or both? An examination of the construct validity of verbal fluency measures. Appl Neuropsychol Adult. 2019;26(5):441–51.
9. Beck IR, Gagneux-Zurbriggen A, Berres M, Taylor KI, Monsch AU. Comparison of verbal episodic memory measures: Consortium to Establish a Registry for Alzheimer's Disease-Neuropsychological Assessment Battery (CERAD-NAB) versus California Verbal Learning Test (CVLT). Arch Clin Neuropsychol. 2012;27(5):510–9.
10. Bruno D, Grothe MJ, Nierenberg J, Sidtis JJ, Teipel SJ, Pomara N. Output order and variability in free recall are linked to cognitive ability and hippocampal volume in elderly individuals. Neuropsychologia. 2016;80:126–32.
11. Troyer AK, Moscovitch M, Winocur G. Clustering and switching as two components of verbal fluency: evidence from younger and older healthy adults. Neuropsychology. 1997;11(1):138–46.
12. Ter Huurne D, Ramakers I, Possemis N, Banning L, Gruters A, Van Asbroeck S, et al. The accuracy of speech and linguistic analysis in early diagnostics of neurocognitive disorders in a memory clinic setting. Arch Clin Neuropsychol. 2023;38(5):667–76.
13. Possemis N, Ter Huurne D, Banning L, Gruters A, Van Asbroeck S, König A, et al. The reliability and clinical validation of automatically-derived verbal memory features of the verbal learning test in early diagnostics of cognitive impairment.Loewenstein D, editor. J Alzheimers Dis. 2024;97(1):179–91
14. Cho S, Cousins KAQ, Shellikeri S, Ash S, Irwin DJ, Liberman MY, et al. Lexical and Acoustic Speech Features Relating to Alzheimer Disease Pathology. Neurology. 2022;99(4).
15. Fristed E, Skirrow C, Meszaros M, Lenain R, Meepegama U, Papp KV, et al. Leveraging speech and artificial intelligence to screen for early Alzheimer's disease and amyloid beta positivity. Brain Commun. 2022;4(5):fcac231.
16. Alexopoulou ZS, Köhler S, Mallick E, Tröger J, Linz N, Spruth E, et al. Speech-based digital cognitive assessments for detection of mild cognitive impairment: Validation against paper-based neurocognitive assessment scores. J Alzheimer's Dis. 2025;108(1):118–131
17. Li Q, Koehler S, Koenig A, Dyrba M, Mallik E, Linz N, et al. Associations between digital speech features of automated cognitive tasks and trajectories of brain atrophy and cognitive decline in early Alzheimer's disease. J Alzheimer's Dis. 2025;107(1):154–169.
18. Jacobs HIL, Radua J, Lückmann HC, Sack AT. Meta-analysis of functional network alterations in Alzheimer's disease: toward a network biomarker. Neurosci Biobehav Rev. 2013;37(5):753–65.
19. Yu E, Liao Z, Tan Y, Qiu Y, Zhu J, Han Z, et al. High-sensitivity neuroimaging biomarkers for the identification of amnestic mild cognitive impairment based on resting-state fMRI and a triple network model. Brain Imaging Behav. 2019;13(1):1–14.
20. Cole DM, Smith SM, Beckmann CF. Advances and pitfalls in the analysis and interpretation of resting-state FMRI data. Front Syst Neurosci. 2010;4:8.
21. Rosazza C, Minati L. Resting-state brain networks: literature review and clinical applications. Neurol Sci. 2011;32(5):773–85.
22. Agosta F, Pievani M, Geroldi C, Copetti M, Frisoni GB, Filippi M. Resting state fMRI in Alzheimer's disease: beyond the default mode network. Neurobiol Aging. 2012;33(8):1564–78.
23. Amaefule CO, Dyrba M, Wolfsgruber S, Polcher A, Schneider A, Fliessbach K, et al. Association between composite scores of domain-specific cognitive functions and regional patterns of atrophy and functional connectivity in the Alzheimer's disease spectrum. Neuroimage Clin. 2021;29:102533.
24. Liang P, Wang Z, Yang Y, Jia X, Li K. Functional disconnection and compensation in mild cognitive impairment: evidence from DLPFC connectivity using resting-state fMRI. He Y, editor. PLoS One. 2011;6(7):e22153.
25. Pistono A, Senoussi M, Guerrier L, Rafiq M, Giméno M, Péran P, et al. Language network connectivity increases in early Alzheimer's disease. J Alzheimers Dis. 2021;82(1):447–60.
26. Teipel SJ, the DELCODE study group, Metzger CD, Brosseron F, Buerger K, Brueggen K, et al. Multicenter resting state functional connectivity in prodromal and dementia stages of Alzheimer's disease. J Alzheimers Dis. 2018;64(3):801–13.
27. Badhwar A, Tam A, Dansereau C, Orban P, Hoffstaedter F, Bellec P. Resting-state network dysfunction in Alzheimer's disease: a systematic review and meta-analysis. Alzheimers Dement. 2017;8(1):73–85.
28. Wang Y, Li Q, Yao L, He N, Tang Y, Chen L, et al. Shared and differing functional connectivity abnormalities of the default mode network in mild cognitive impairment and Alzheimer's disease. Cereb Cortex. 2024;34(3):bhae094.
29. Celebi O, Uzdogan A, Oguz KK, Has AC, Dolgun A, Cakmakli GY, et al. Default mode network connectivity is linked to cognitive functioning and CSF Aβ1–42 levels in Alzheimer's disease. Arch Gerontol Geriatr. 2016;62:125–32.
30. Han SD, Arfanakis K, Fleischman DA, Leurgans SE, Tuminello ER, Edmonds EC, et al. Functional connectivity variations in mild cognitive

impairment: associations with cognitive function. J Int Neuropsychol Soc. 2012;18(1):39–48.
31. Petrella JR, Sheldon FC, Prince SE, Calhoun VD, Doraiswamy PM. Default mode network connectivity in stable vs progressive mild cognitive impairment. Neurology. 2011;76(6):511–7.
32. Mascali D, DiNuzzo M, Serra L, Mangia S, Maraviglia B, Bozzali M, et al. Disruption of semantic network in mild Alzheimer's disease revealed by resting-state fMRI. Neuroscience. 2018;371:38–48.
33. König A, Linz N, Baykara E, Tröger J, Ritchie C, Saunders S, et al. Screening over Speech in Unselected Populations for Clinical Trials in AD (PROSPECT-AD): Study Design and Protocol. J Prev Alzheimers Dis. 2023;10(2):314–321.
34. Jessen F, Spottke A, Boecker H, Brosseron F, Buerger K, Catak C, et al. Design and first baseline data of the DZNE multicenter observational study on predementia Alzheimer's disease (DELCODE). Alzheimers Res Ther. 2018;10(1):15.
35. Jessen F, Amariglio RE, Van Boxtel M, Breteler M, Ceccaldi M, Chételat G, et al. A conceptual framework for research on subjective cognitive decline in preclinical Alzheimer's disease. Alzheimers Dement. 2014;10(6):844–52.
36. Albert MS, DeKosky ST, Dickson D, Dubois B, Feldman HH, Fox NC, et al. The diagnosis of mild cognitive impairment due to Alzheimer's disease: recommendations from the National Institute on Aging-Alzheimer's Association workgroups on diagnostic guidelines for Alzheimer's disease. Alzheimers Dement. 2011;7(3):270–9.
37. McKhann GM, Knopman DS, Chertkow H, Hyman BT, Jack CR, Kawas CH, et al. The diagnosis of dementia due to Alzheimer's disease: recommendations from the National Institute on Aging-Alzheimer's Association workgroups on diagnostic guidelines for Alzheimer's disease. Alzheimers Dement. 2011;7(3):263–9.
38. König A, Köhler S, Tröger J, Düzel E, Glanz W, Butryn M, et al. Automated remote speech-based testing of individuals with cognitive decline: Bayesian agreement of transcription accuracy. Alzheimer's & Dementia: Diagnosis, Assessment & Disease Monitoring. 2024;16(4):e70011.
39. Tröger J, Baykara E, Zhao J, Ter Huurne D, Possemis N, Mallick E, et al. Validation of the Remote Automated ki:e Speech Biomarker for Cognition in Mild Cognitive Impairment: verification and validation following DiME V3 framework. Digit Biomark. 2022;6(3):107–16.
40. Vita MG, Marra C, Spinelli P, Caprara A, Scaricamazza E, Castelli D, et al. Typicality of words produced on a semantic fluency task in amnesic mild cognitive impairment: linguistic analysis and risk of conversion to dementia. J Alzheimers Dis. 2014;42(4):1171–8.
41. Tröger J, Linz N, König A, Robert P, Alexandersson J, Peter J, et al. Exploitation vs. exploration—computational temporal and semantic analysis explains semantic verbal fluency impairment in Alzheimer's disease. Neuropsychologia. 2019;131:53–61.
42. Estévez-González A, Kulisevsky J, Boltes A, Otermín P, García-Sánchez C. Rey verbal learning test is a useful tool for differential diagnosis in the preclinical phase of Alzheimer's disease: comparison with mild cognitive impairment and normal aging. Int J Geriatr Psychiatry. 2003;18(11):1021–8.
43. Meijs C, Hurks P, Rozendaal N, Jolles J. Serial and subjective clustering on a verbal learning test (VLT) in children aged 5–15: the nature of subjective clustering. Child Neuropsychol. 2013;19(4):385–99.
44. Chao-Gan Y, Yu-Feng Z. DPARSF: A MATLAB Toolbox for "Pipeline" Data Analysis of Resting-State fMRI. Front Syst Neurosci. 2010;4:13.
45. Ashburner J. A fast diffeomorphic image registration algorithm. Neuroimage. 2007;38(1):95–113.
46. Jenkinson M, Bannister P, Brady M, Smith S. Improved optimization for the robust and accurate linear registration and motion correction of brain images. Neuroimage. 2002;17(2):825–41.
47. Abou-Elseoud A, Starck T, Remes J, Nikkinen J, Tervonen O, Kiviniemi V. The effect of model order selection in group PICA. Hum Brain Mapp. 2010;31(8):1207–16.
48. Mikl M, Mareček R, Hluštík P, Pavlicová M, Drastich A, Chlebus P, et al. Effects of spatial smoothing on fMRI group inferences. Magn Reson Imaging. 2008;26(4):490–503.
49. Shirer WR, Ryali S, Rykhlevskaia E, Menon V, Greicius MD. Decoding subject-driven cognitive states with whole-brain connectivity patterns. Cereb Cortex. 2012;22(1):158–65.
50. Smith SM, Fox PT, Miller KL, Glahn DC, Fox PM, Mackay CE, et al. Correspondence of the brain's functional architecture during activation and rest. Proc Natl Acad Sci USA. 2009;106(31):13040–5.
51. Beckmann C, Mackay C, Filippini N, Smith S. Group comparison of resting-state FMRI data using multi-subject ICA and dual regression. Neuroimage. 2009;47:S148.
52. Nickerson LD, Smith SM, Öngür D, Beckmann CF. Using dual regression to investigate network shape and amplitude in functional connectivity analyses. Front Neurosci. 2017;11:115.
53. R Core Team. R: A language and environment for statistical computing. Vienna, Austria: R Foundation for Statistical Computing; 2018. Available from: https://www.R-project.org/.
54. Smith S, Nichols T. Threshold-free cluster enhancement: addressing problems of smoothing, threshold dependence and localisation in cluster inference. Neuroimage. 2009;44(1):83–98.
55. Davey J, Thompson HE, Hallam G, Karapanagiotidis T, Murphy C, De Caso I, et al. Exploring the role of the posterior middle temporal gyrus in semantic cognition: integration of anterior temporal lobe with executive processes. Neuroimage. 2016;137:165–77.
56. Park LQ, Gross AL, McLaren DG, Pa J, Johnson JK, et al. Confirmatory factor analysis of the ADNI neuropsychological battery. Brain Imaging Behav. 2012;6(4):528–39.
57. Jutten RJ, Harrison JE, Brunner AJ, Vreeswijk R, Van Deelen RAJ, De Jong FJ, et al. The cognitive-functional composite is sensitive to clinical progression in early dementia: longitudinal findings from the catch-cog study cohort. Alzheimers Dement Transl Res Clin Interv. 2020;6(1):e12020.
58. Yue C, Wu D, Bai F, Shi Y, Yu H, Xie C, et al. State-based functional connectivity changes associate with cognitive decline in amnestic mild cognitive impairment subjects. Behav Brain Res. 2015;288:94–102.
59. Donohue MC, Sperling RA, Salmon DP, Rentz DM, Raman R, Thomas RG, et al. The Preclinical Alzheimer Cognitive Composite: Measuring Amyloid-Related Decline. JAMA Neurol. 2014;71(8):961.
60. Burnham SC, Bourgeat P, Doré V, Savage G, Brown B, Laws S, et al. Clinical and cognitive trajectories in cognitively healthy elderly individuals with suspected non-Alzheimer's disease pathophysiology (SNAP) or Alzheimer's disease pathology: a longitudinal study. Lancet Neurol. 2016;15(10):1044–53.
61. Mormino EC, Papp KV, Rentz DM, Donohue MC, Amariglio R, Quiroz YT, et al. Early and late change on the preclinical Alzheimer's cognitive composite in clinically normal older individuals with elevated amyloid β. Alzheimers Dement. 2017;13(9):1004–12.
62. Kemik K, Ada E, Çavuşoğlu B, Aykaç C, Savaş DDE, Yener G. Detecting language network alterations in mild cognitive impairment using task-based fMRI and resting-state fMRI: A comparative study. Brain Behav. 2024;14(5):e3518.
63. Marek S, Tervo-Clemmens B, Calabro FJ, Montez DF, Kay BP, Hatoum AS, et al. Reproducible brain-wide association studies require thousands of individuals. Nature. 2022;603(7902):654–60.
64. Li MT, Sun JW, Zhan LL, Antwi CO, Lv YT, Jia XZ, et al. The effect of seed location on functional connectivity: evidence from an image-based meta-analysis. Front Neurosci. 2023;17:1120741

Publisher's Note

Springer Nature remains neutral with regard to jurisdictional claims in published maps and institutional affiliations.